

Interaction of Ethynyliron (Fp-C≡C-H and Fp*-C≡C-H) and Ethynediyliron Complexes (Fp*-C≡C-Fp*) with Co₂(CO)₈: Formation of a Cluster Compound Which Is Fluxional via a Metal-Metal Bond Scission and Recombination Process[†]

Munetaka Akita,* Masako Terada, and Yoshihiko Moro-oka*

Research Laboratory of Resources Utilization, Tokyo Institute of Technology,
4259 Nagatsuta, Midori-ku, Yokohama 227, Japan

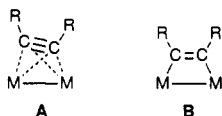
Received November 15, 1991

Interaction of ethynyliron complexes Fp-C≡C-H (1) and Fp*-C≡C-H (2) with Co₂(CO)₈ in THF results in the respective formation of the expected deep green adducts with a tetrahedral C₂Co₂ core, Co₂(CO)₆(μ-η²:η²-M-C≡C-H) (3, M = Fp; 4, M = Fp*). The structural features of 3 and 4 characterized by spectroscopic (and crystallographic) analyses are essentially the same as those of adducts derived from normal alkynes, Co₂(CO)₆(μ-η²:η²-R-C≡C-R'). The reaction of the ethynediyliron complex Fp*-C≡C-Fp* (7) with Co₂(CO)₈ similarly affords the deep green adduct Cp*Fe[Co(CO)₂]₂(μ-CO)₂(μ-η¹:η²:η²-C≡C-Fp*) (8), which turns out to be fluxional at ambient temperature. The crystallographic analysis has revealed that the C₂ ligand in 8 binds the four metal atoms together in a μ₄-η¹(Fe):η¹(Fe):η²(Co):η²(Co) fashion; in other words, the bridging C₂ ligand interacts with a remote iron atom in an η¹(σ) fashion and with the remaining FeCo₂ cluster part in a μ₃-η¹(Fe):η²(Co):η²(Co) fashion, respectively. A rare example of fluxional behavior of 8 via a metal-metal bond scission and recombination process has been studied by variable-temperature ¹³C NMR analyses, and below -60 °C spectra consistent with the solid-state structure have been obtained. Crystal data: 3, triclinic, space group P $\bar{1}$, Z = 2, a = 9.798 (1) Å, b = 13.082 (3) Å, c = 7.765 (1) Å, α = 95.06 (2)°, β = 114.10 (1)°, γ = 97.54 (2)°, V = 889.5 (3) Å³, R (R_w) = 0.050 (0.043) for 2632 reflections with I > 3σ(I); 8, monoclinic, space group C2/c, Z = 8, a = 33.095 (9) Å, b = 10.131 (3) Å, c = 20.572 (7) Å, β = 113.19 (92)°, V = 6340 (4) Å³, R (R_w) = 0.081 (0.071) for 1524 reflections with I > 3σ(I).

Introduction

Alkyne and alkynyl species bearing a C≡C functional group belong to a class of surface species which may play a pivotal role in various catalytic reactions such as CO hydrogenation, and the coordination chemistry of the corresponding ligands has been studied extensively.¹ However, little information on chemical properties of parent acetylide complexes, i.e. ethynylmetal complexes (M-C≡C-H)² and ethynediylmetal complexes (M-C≡C-M),³ has been available probably because of the limited accessibility of the starting compounds, whereas they appear to be closer to the real surface species than those with an organic substituent. In a previous paper^{3a} we reported the preparation of the cationic diiron μ-η¹:η²-ethynyl complex [Fp*₂(C≡C-H)]BF₄ by the reaction of the ethynyliron complex Fp*-C≡C-H with a mononuclear cationic species (Fp*⁺). The resulting cationic dinuclear complex showed an unprecedented prototropic fluxional behavior⁴ and was readily deprotonated to give an ethynediyliron complex, Fp*-C≡C-Fp*.⁵ These results prompted us to examine adduct formation of the parent iron acetylide complexes with dinuclear species.

The interaction of alkyne with dinuclear species leading to adducts with a tetrahedral C₂M₂ core (A) or a dimetallacyclobutene structure (B) has been recognized as one of the classical reactions in the field of organometallic chemistry.^{1,6} However, application of this reaction to



metal acetylide complexes has been studied less extensively. In 1972 Yamazaki et al. first reported the prepara-

tion of di- and trinuclear adducts derived from Ti, Fe, and Ni acetylides,⁷ and one of the products, namely Co₂-

(1) (a) Collman, J. P.; Hegedus, L. S.; Norton, J. R.; Finke, R. G. *Principles and Applications of Organotransition Metal Chemistry*, 2nd ed.; University Science Books: Mill Valley, CA, 1987. (b) Sappa, E.; Tiripicchio, A.; Braunstein, P. *Chem. Rev.* 1983, 83, 203.

(2) (a) M = Fp*: Akita, M.; Terada, M.; Oyama, S.; Moro-oka, Y. *Organometallics* 1990, 9, 816. (b) M = Fp: Kim, P. J.; Masai, H.; Sonogashira, K.; Hagihara, N. *Inorg. Nucl. Chem. Lett.* 1970, 6, 181. (c) M = CpFe(dppe): Davison, A.; Selegue, J. P. *J. Am. Chem. Soc.* 1978, 100, 7763. (d) M = CpFe(CO)(PPh₃): Boland-Lussier, B. E.; Churchill, M. R.; Hughes, R. P.; Rheingold, A. L. *Organometallics* 1982, 1, 628. (e) M = CpFe(dppm): Gamasa, M. P.; Gimeno, J.; Lastra, E.; Lanfranchi, M.; Tiripicchio, A. *J. Organomet. Chem.* 1991, 405, 333. (f) M = group 11 metal: Nast, R. *Coord. Chem. Rev.* 1982, 47, 89. (g) M = CpNi(PPh₃): Yamazaki, H.; Nishido, Y.; Matsumoto, Y.; Sumida, S.; Hagihara, N. *J. Organomet. Chem.* 1966, 6, 86. (h) M = CpNi(PPh₃), Pd(PR₃)₂X, Pt(PR₃)₂X: Sonogashira, K.; Fujikura, Y.; Yatake, T.; Toyoshima, N.; Takahashi, S.; Hagihara, N. *J. Chem. Soc., Chem. Commun.* 1977, 291. (i) M = Pt(PR₃)₂X: Bell, R. A.; Chisholm, M.; Cough, D. A.; Rankel, L. A. *Inorg. Chem.* 1977, 16, 677. (k) M = Re(CO)₅: Appel, M.; Heidrich, J.; Beck, W. *Chem. Ber.* 1987, 120, 1087. (l) M = Rh⁺[N(CH₂CH₂PPh₃)₃](H), Rh⁺[P(CH₂CH₂PPh₃)₃](H): Bianchini, C.; Masi, D.; Meli, A.; Peruzzini, M.; Ramirez, J. A. *Organometallics* 1989, 8, 2179.

(3) Recently an increasing number of examples have been reported. (a) M = Fp*: Reference 2a. (b) M = CpRu(CO)₂: Koutsantonis, G.; Selegue, J. P. *J. Am. Chem. Soc.* 1991, 113, 2316. (c) M = Ru-W, Fe-W: Frank, K. G.; Selegue, J. P. *J. Am. Chem. Soc.* 1990, 112, 6414. (d) M = Pd(PR₃)₂X, Pt(PR₃)₂X: Ogawa, H.; Onitsuka, K.; Joh, T.; Takahashi, K.; Yamazaki, H. *Organometallics* 1988, 7, 2257. (e) M = Re(CO)₅: see ref 2k. (f) Heidrich, J.; Steimann, M.; Appel, M.; Beck, W.; Phillips, J. R.; Troglor, W. C. *Organometallics* 1990, 9, 1296. (g) M = CpW(CO)₃: Chan, M.-C.; Tsai, Y.-J.; Chen, C.-T.; Lin, Y.-C.; Tseng, T.-W.; Lee, G.-H.; Wang, Y. *Organometallics* 1991, 10, 378. (h) M = Cp*₂Sc: St. Clair, M.; Schaefer, W. P.; Bercaw, J. E. *Organometallics* 1991, 10, 525. (i) M = Mn(CO)₅: Davis, J. A.; El-Ghanam, M.; Pinckerton, A. A.; Smith, D. A. *J. Organomet. Chem.* 1991, 409, 367. (j) See also references cited in ref 3b.

(4) Silvestre, J.; Hoffmann, R. *Helv. Chim. Acta* 1985, 68, 1461.

(5) (a) Akita, M.; Terada, M.; Oyama, S.; Sugimoto, S.; Moro-oka, Y. *Organometallics* 1991, 10, 1561. (b) Akita, M.; Terada, M.; Moro-oka, Y. *Organometallics* 1991, 10, 2962.

(6) Hoffman, D. M.; Hoffmann, R.; Fisel, C. R. *J. Am. Chem. Soc.* 1982, 104, 3858.

[†] Abbreviations: Fp = CpFe(CO)₂; Cp = η⁵-C₅H₅; Fp* = Cp*Fe(CO)₂; Cp* = η⁵-C₅Me₅.

Table I. Crystallographic Data for 3 and 8

	3	8
formula	C ₁₅ H ₆ O ₈ FeCo ₂	C ₃₀ H ₃₀ O ₈ Fe ₂ Co ₂
fw	487.91	748.10
space group	triclinic, P $\bar{1}$	monoclinic, C2/c
a, Å	9.798 (1)	33.095 (9)
b, Å	13.082 (3)	10.131 (3)
c, Å	7.765 (1)	20.572 (7)
α , deg	95.06 (2)	
β , deg	114.10 (1)	113.19 (2)
γ , deg	97.54 (2)	
V, Å ³	889.5 (3)	6340 (4)
Z	2	8
d_{calc} , g cm ⁻³	1.822	1.568
μ , cm ⁻¹	27.0	19.7
2 θ , deg	2-55	2-45
no. of data collected	4379	4723
no. of data with $I > 3\sigma(I)$	2632	1524
no. of variables	252	278
R	0.050	0.088
R _w	0.043	0.071

Table II. Positional Parameters and B_{eq} Values for 3

atom	x	y	z	B_{eq} , Å ²
CP ^a	0.42489	0.20975	-0.35274	
Fe	0.54073 (5)	0.24098 (3)	-0.11028 (6)	4.18 (1)
Co1	0.93548 (5)	0.37305 (2)	0.20806 (6)	4.09 (1)
Co2	0.93668 (5)	0.19608 (3)	0.06534 (6)	5.14 (1)
C1	0.7612 (3)	0.2779 (2)	-0.0201 (4)	3.7 (1)
C2	0.8741 (4)	0.3156 (2)	-0.0581 (4)	4.2 (1)
C3	0.4498 (8)	0.1285 (4)	-0.3585 (7)	8.0 (2)
C4	0.5284 (5)	0.2098 (6)	-0.3871 (6)	7.5 (2)
C5	0.4703 (7)	0.2986 (4)	-0.3679 (7)	8.3 (2)
C6	0.3413 (6)	0.2591 (6)	-0.3296 (6)	9.6 (2)
C7	0.3346 (6)	0.1528 (5)	-0.3206 (7)	8.3 (2)
C11	0.5381 (4)	0.3458 (3)	0.0499 (5)	5.3 (1)
C12	0.5557 (4)	0.1551 (3)	0.0541 (5)	5.3 (1)
C13	0.8865 (4)	0.3361 (3)	0.3922 (5)	6.7 (2)
C14	1.1344 (4)	0.4249 (3)	0.2987 (5)	5.2 (1)
C15	0.8689 (4)	0.4938 (3)	0.1728 (5)	6.0 (1)
C16	0.9285 (5)	0.1277 (3)	0.2442 (7)	8.4 (2)
C17	1.1319 (5)	0.2115 (3)	0.0968 (6)	7.4 (3)
C18	0.8530 (5)	0.0956 (4)	-0.1260 (8)	9.8 (2)
O11	0.5363 (3)	0.4124 (2)	0.1531 (4)	8.3 (1)
O12	0.5648 (3)	0.1002 (2)	0.1630 (4)	8.6 (1)
O13	0.8465 (4)	0.3092 (3)	0.5032 (4)	11.7 (2)
O14	1.2600 (3)	0.4601 (2)	0.3519 (4)	8.2 (1)
O15	0.8248 (3)	0.5687 (2)	0.1442 (4)	9.2 (1)
O16	0.9257 (4)	0.0830 (3)	0.3667 (6)	13.6 (2)
O17	1.2539 (3)	0.2207 (3)	0.1156 (5)	11.6 (2)
O18	0.7929 (4)	0.0288 (3)	-0.2533 (6)	15.6 (2)
H2	0.895 (3)	0.346 (2)	-0.173 (4)	3.85
H3	0.461 (5)	0.053 (3)	-0.362 (6)	7.94
H4	0.625 (4)	0.210 (3)	-0.417 (5)	7.10
H5	0.522 (5)	0.369 (3)	-0.375 (6)	8.48
H6	0.281 (5)	0.291 (3)	-0.318 (6)	9.45
H7	0.242 (5)	0.090 (3)	-0.318 (6)	8.06

^aCP is the centroid of the Cp ring (C3-C7).

(CO)₆(μ - η^2 : η^2 -Fp-C \equiv C-Ph), was later structurally characterized by Bruce et al.⁸ In addition, the Fe and Ru analogues were afterwards found by Vahrenkamp et al.⁹ to be oxidatively converted to trinuclear μ_3 -alkylidyne complexes. Very recently Beck et al. reported reaction of an ethynediylrhenium complex, (OC)₅Re-C \equiv C-Re(CO)₅, with mono- and dinuclear species.¹⁰

(7) (a) Yasufuku, K.; Yamazaki, H. *Bull. Chem. Soc. Jpn.* 1972, 45, 2664. (b) Yasufuku, K.; Aoki, K.; Yamazaki, H. *Bull. Chem. Soc. Jpn.* 1975, 48, 1616.

(8) Bruce, M. I.; Duffy, D. N.; Humphrey, M. G. *Aust. J. Chem.* 1986, 39, 159.

(9) (a) Bernhardt, W.; Vahrenkamp, H. *Organometallics* 1986, 5, 2388. (b) Bernhardt, W.; Vahrenkamp, H. *J. Organomet. Chem.* 1990, 383, 357.

(10) Weidmann, T.; Weinrich, V.; Wagner, B.; Robl, C.; Beck, W. *Chem. Ber.* 1991, 124, 1363.

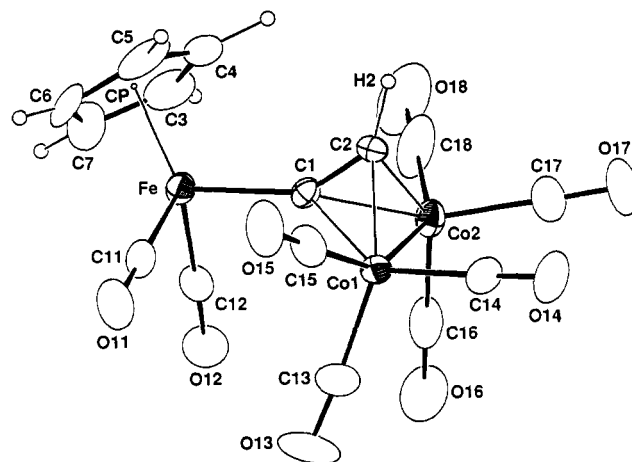


Figure 1. ORTEP view of 3 drawn at the 30% probability level.

Table III. Structure Parameters for Co₂(CO)₆(μ - η^2 : η^2 -R-C \equiv C-R')^a

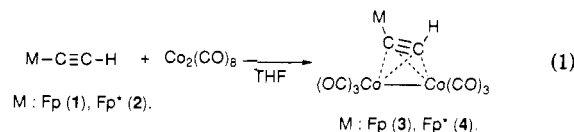
	R-C \equiv C-R'		
	Fp-C \equiv C-H (3)	Fp-C \equiv C-Ph (5) ^b	Bu ⁺ -C \equiv C-Bu ⁺ (6) ¹⁴
C1-C2	1.305 (5)	1.32 (2)	1.341 (3)
C1-Fe	1.954 (3)	1.99 (1)	
C1-Co1	2.046 (2)	2.03 (1)	1.988 (2)
C1-Co2	2.054 (3)	1.98 (1)	1.992 (2)
C2-H2	1.09 (4)		
C2-Co1	1.943 (3)	1.97 (1)	1.982 (2)
C2-Co2	1.947 (3)	1.97 (1)	1.985 (2)
Co1-Co2	2.481 (1)	2.478 (2)	2.460 (2)
Fe-C11	1.778 (4)	1.78 (2)	
Fe-C12	1.748 (4)	1.82 (2)	
C11-O11	1.137 (5)		
C12-O12	1.141 (5)		
Co1-CO	1.769 (5), 1.787 (4), 1.790 (4)	1.80, 1.81, 1.83 (2)	1.790 (2), 1.812 (2), 1.826 (2)
Co2-CO	1.728 (5), 1.739 (6), 1.808 (5)	1.74, 1.80, 1.83 (2)	1.788 (3), 1.822 (2), 1.828 (2)
\angle Fe-C1-C2	146.9 (2)	142.9 (10)	144.1 (2)
\angle C1-C2-H2	140 (1)	141.0 (12)	144.8 (2)

^aBond lengths are in angstroms and bond angles in degrees.

Herein we wish to report adduct formation of ethynyliron (Fp-C \equiv C-H and Fp*-C \equiv C-H) and ethynediyliron complexes (Fp*-C \equiv C-Fp*) with Co₂(CO)₆¹¹ and an unusual fluxional property of the latter adduct.

Results and Discussion

Interaction of Ethynyliron Complexes with Co₂(C-O)₆. Reaction of the ethynyliron complexes Fp-C \equiv C-H (1) and Fp*-C \equiv C-H (2) with Co₂(CO)₆ in THF smoothly proceeded with gas evolution to afford deep green adducts 3 and 4 in 83% and 70% yield, respectively (eq 1). The structure of the adducts characterized by means



of spectroscopic and crystallographic analyses contains a tetrahedral C₂Co₂ core (structure A), which has been widely established for the well-known alkyne adducts Co₂(CO)₆(μ - η^2 : η^2 -R-C \equiv C-R').¹¹ The ¹³C NMR parameters of the bridging C₂H part fall in the range of those of the usual organic counterparts (δ 70-100; ¹J_{C-H} \approx 220 Hz).^{12,13} Thus,

(11) Dickson, R. S.; Fraser, P. J. *Adv. Organomet. Chem.* 1974, 12, 323.

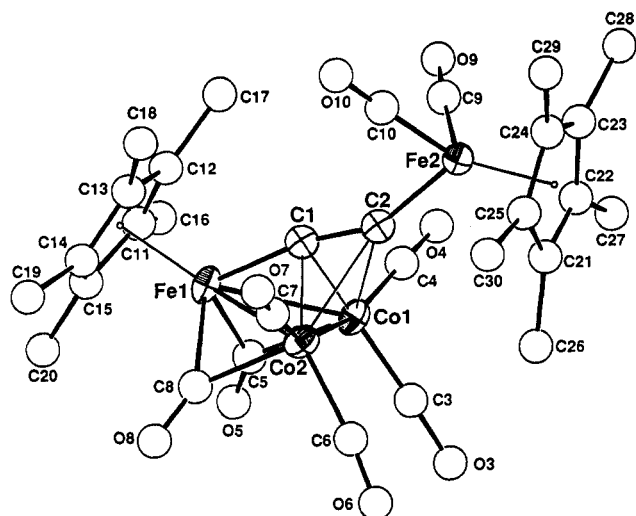
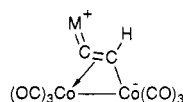
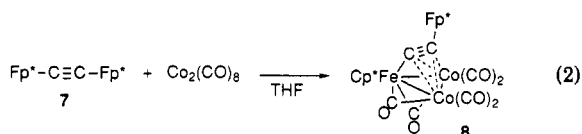


Figure 2. ORTEP view of **8** with C and O atoms drawn with an arbitrary size.

introduction of an Fp or Fp* group as an alkyne substituent does not result in a significant shift of $\delta(\text{C}-\text{Fe})$, while $\delta(\text{C}-\text{H})$'s (95.7 (1), 92.6 (2)) are observed at lower field than those of the $\text{R}-\text{C}\equiv\text{C}-\text{H}$ derivatives ($\delta(\text{C}-\text{H}) = 71-74$).¹² The molecular structure of **3** (Figure 1) has been determined by X-ray crystallography, and the crystallographic data and positional parameters are summarized in Tables I and II. As indicated by the spectroscopic analyses, the overall core structure of **3** is essentially the same as those of the $\text{Fp}-\text{C}\equiv\text{C}-\text{Ph}$ (**5**) and $\text{Bu}^t-\text{C}\equiv\text{C}-\text{Bu}^t$ (**6**)¹⁴ adducts (Table III).¹¹ On coordination the Fp and H parts bend away from the original linear structure ($\angle\text{Fe1}-\text{C1}-\text{C2}$, 146.9 (2)°; $\angle\text{C1}-\text{C2}-\text{H2}$, 140 (1)°), and the $\text{C}\equiv\text{C}$ and $\text{Fe}-\text{C}\equiv$ distances are elongated by ca. 0.13 and ca. 0.03 Å, respectively, when compared with those of $\text{Fp}^*-\text{C}\equiv\text{C}-\text{H}$ (**2**) ($\text{C}\equiv\text{C}$, 1.173 (4) Å, $\text{Fe}-\text{C}\equiv$, 1.921 (3) Å).^{2a} The most significant feature is that C2 lies closer to the Co atoms than C1 does by ca. 0.1 Å, whereas the four C-Co distances of the previous examples are the same within experimental errors¹¹ (cf. **5** and **6**). In addition, the $\text{C}\equiv\text{C}$ and $\text{C}=\text{O}$ lengths in **3** are slightly shorter than those in the previously reported analogues. These structural features may be partly explained by the steric or electron-donating effect of the Fp group or one of the limiting resonance structures



Interaction of $\text{Fp}^*-\text{C}\equiv\text{C}-\text{Fp}^*$ (2**) with $\text{Co}_2(\text{CO})_8$ and Fluxional Behavior of the Adduct.** The ethynediyliron complex $\text{Fp}^*-\text{C}\equiv\text{C}-\text{Fp}^*$ (**7**) readily reacted with $\text{Co}_2(\text{CO})_8$ also, and the deep green adduct **8** was isolated in 76% yield as the sole product after simple crystallization (eq 2). Since the ¹³C NMR spectrum recorded



(12) Aime, S.; Milone, L.; Rossetti, R.; Stanghellini, P. L. *Inorg. Chim. Acta* 1977, 22, 135.

(13) Mann, B. E.; Taylor, B. F. *¹³C-NMR Data for Organometallic Compounds*; Academic: New York, 1981.

(14) Gregson, D.; Howard, J. A. K. *Acta Crystallogr.* 1983, C39, 1024.

Table IV. Positional Parameters and B_{eq} Values for **8**

atom	x	y	z	B_{eq} , Å ²
CP1 ^a	0.12038	0.45624	0.44078	
CP2 ^a	0.12568	0.07299	0.76651	
Co1	0.17145 (9)	0.1275 (3)	0.5641 (2)	4.1 (1)
Co2	0.08998 (9)	0.1048 (3)	0.5089 (2)	4.0 (1)
Fe1	0.12527 (9)	0.2946 (3)	0.4718 (2)	3.8 (1)
Fe2	0.1258 (1)	0.2040 (3)	0.7112 (2)	4.0 (1)
C1	0.1245 (5)	0.253 (2)	0.561 (1)	3.2 (7)
C2	0.1275 (6)	0.198 (2)	0.622 (1)	4.1 (8)
C3	0.1881 (8)	-0.029 (3)	0.565 (1)	7 (1)
C4	0.2217 (8)	0.177 (2)	0.628 (1)	5.2 (9)
C5	0.1714 (6)	0.182 (2)	0.471 (1)	5 (1)
C6	0.0899 (8)	-0.071 (2)	0.497 (1)	5 (1)
C7	0.0339 (7)	0.139 (2)	0.497 (1)	5.1 (9)
C8	0.0873 (6)	0.153 (2)	0.412 (1)	4.0 (9)
C9	0.1674 (8)	0.321 (3)	0.734 (1)	7 (1)
C10	0.0821 (8)	0.324 (3)	0.679 (1)	6 (1)
C11	0.1582 (7)	0.460 (2)	0.458 (1)	5 (1)
C12	0.1393 (7)	0.495 (2)	0.502 (1)	4 (1)
C13	0.0928 (7)	0.477 (2)	0.461 (1)	4 (1)
C14	0.0847 (7)	0.429 (2)	0.394 (1)	5 (1)
C15	0.1270 (6)	0.420 (2)	0.389 (1)	4 (1)
C16	0.2114 (7)	0.476 (2)	0.479 (1)	6 (1)
C17	0.1593 (7)	0.548 (2)	0.577 (1)	5 (1)
C18	0.0565 (7)	0.508 (2)	0.490 (1)	6 (1)
C19	0.0405 (7)	0.412 (2)	0.334 (1)	7 (1)
C20	0.1343 (7)	0.378 (3)	0.327 (1)	8 (1)
C21	0.1290 (8)	-0.011 (2)	0.725 (1)	6 (1)
C22	0.1639 (7)	0.054 (2)	0.778 (1)	5 (1)
C23	0.1459 (7)	0.140 (2)	0.816 (1)	4 (1)
C24	0.1015 (7)	0.135 (2)	0.786 (1)	6 (1)
C25	0.0882 (7)	0.046 (2)	0.728 (1)	5 (1)
C26	0.1330 (7)	-0.116 (2)	0.675 (1)	7 (1)
C27	0.2128 (8)	0.024 (2)	0.800 (1)	7 (1)
C28	0.1719 (7)	0.211 (3)	0.883 (1)	8 (1)
C29	0.0683 (7)	0.196 (2)	0.810 (1)	8 (1)
C30	0.0420 (8)	0.003 (2)	0.679 (1)	7 (1)
O3	0.2013 (6)	-0.143 (2)	0.564 (1)	8.7 (8)
O4	0.2544 (5)	0.208 (2)	0.6733 (9)	8.4 (7)
O5	0.1926 (5)	0.151 (2)	0.4398 (8)	7.8 (7)
O6	0.0873 (6)	-0.181 (2)	0.483 (1)	9.4 (8)
O7	0.0003 (5)	0.166 (2)	0.495 (1)	10.6 (8)
O8	0.0701 (5)	0.114 (2)	0.356 (8)	7.7 (7)
O9	0.1972 (6)	0.392 (2)	0.751 (1)	9.6 (9)
O10	0.0553 (6)	0.398 (2)	0.660 (1)	12 (1)

^aCP1 and CP2 are the centroids of the Cp* rings C11-C15 and C21-C25, respectively.

Table V. Selected Structural Parameters for **8**

Bond Lengths			
C1-C2	1.34 (3)	C1-Fe1	1.89 (2)
C1-Co1	1.98 (2)	C1-Co2	1.93 (2)
C2-Fe2	1.86 (3)	C2-Co1	2.33 (3)
C2-Co2	2.36 (2)	Fe1-Co1	2.553 (4)
Fe1-Co2	2.520 (5)	Co1-Co2	2.490 (4)
Fe1-C5	1.91 (2)	Co1-C5	1.98 (3)
Fe1-C8	1.98 (2)	Co2-C8	2.02 (3)
Co1-CO	1.67 (3)	Co2-CO	1.80 (3)
	1.74 (2)		1.81 (3)
Bond Angles			
$\angle\text{Fe1}-\text{C1}-\text{C2}$	168 (2)	$\angle\text{C1}-\text{C2}-\text{Fe2}$	153 (2)
$\angle\text{C1}-\text{C2}-\text{Fe1}$	153 (2)	$\angle\text{Fe1}-\text{C5}-\text{O5}$	145 (2)
$\angle\text{Co1}-\text{C5}-\text{O5}$	133 (2)	$\angle\text{Fe1}-\text{C8}-\text{O8}$	145 (2)
$\angle\text{Co2}-\text{C8}-\text{O8}$	137 (2)		

at room temperature, containing only one set of Cp* signals, did not provide us with any structural information (see below), the molecular structure of **8** was confirmed by X-ray crystallography (Figure 2). The crystal data, positional parameters, and selected structural parameters are summarized in Tables I, IV, and V. Interaction of the $\text{C}\equiv\text{C}$ part with the four metal centers results in elongation by ca. 0.13 Å when compared with the bond lengths in the starting complex $\text{Fp}^*-\text{C}\equiv\text{C}-\text{Fp}^*$ (**7**) ($\text{Fe}-\text{C}\equiv$, 1.932 (3),

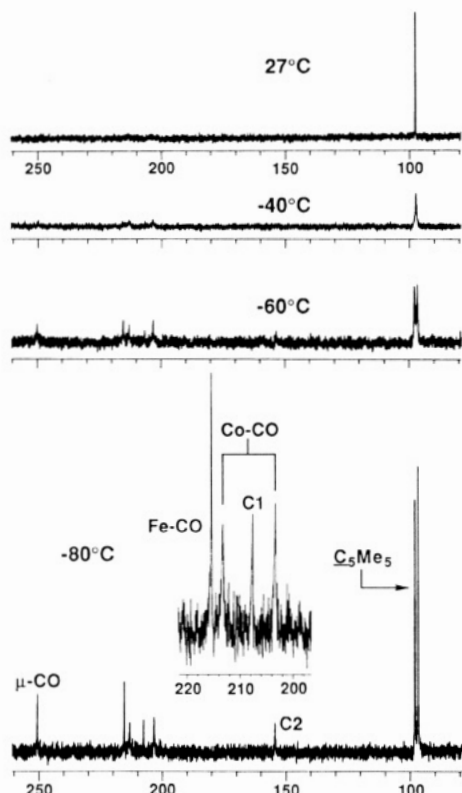
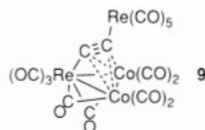


Figure 3. Variable-temperature ^{13}C NMR spectra of **8** observed at 67.9 MHz in CD_2Cl_2 (C_5Me_5 region is omitted for clarity).

1.936 (4) Å; $\text{C}\equiv\text{C}$, 1.209 (4) Å,¹⁵ and the $\text{C}\equiv\text{C}$ length ($\text{C}1-\text{C}2$, 1.34 (3) Å) is still longer than those in the $\text{Fp}-\text{C}\equiv\text{C}-\text{H}$ adduct **3** (1.305 (5) Å), the rhenium analogue $(\text{OC})_3\text{Re}[\text{Co}(\text{CO})_2]_2(\mu-\text{CO})_2[\mu_3-\eta^1(\text{Re}):\eta^2(\text{Co}):\eta^2(\text{Co})-\text{C}\equiv\text{C}-\text{Re}(\text{CO})_5]$ (**9**; 1.28 (2) Å), prepared by a similar route,¹⁰



and the closely related anionic iron cluster compound $\text{PPN}[\text{Fe}_3(\text{CO})_9(\eta_3-\eta^1:\eta^2:\eta^3-\text{C}\equiv\text{C}-\text{Fp})]$ (1.288 (5) Å).¹⁶ In addition, the $\text{Fe}-\text{C}\equiv$ distances in **8** are considerably shortened. Thus, the bridging $\text{C}\equiv\text{C}$ part interacts with the remote Fe atom (Fe2) in a $\eta^1(\sigma)$ fashion and with the remaining FeCo_2 cluster skeleton in a $\mu_3-\eta^1(\text{Fe}1):\eta^2(\text{Co}1):\eta^2(\text{Co}2)$ fashion. The latter is one of the common coordination modes found for trinuclear cluster compounds with a triply bridging alkynyl ligand.^{2b} As a whole, the C_2 ligand binds four metal atoms together in a $\mu_4-\eta^1(\text{Fe}1):\eta^1(\text{Fe}2):\eta^2(\text{Co}1):\eta^2(\text{Co}2)$ fashion. The formation of **8** and the dirhenium analogue (**9**) may be interpreted by the initial formation of a $\mu-\eta^2:\eta^2$ adduct like **3** and **4** followed by decarbonylation leading to metal-metal bond formation.

The inconsistency between the molecular structure and the ^{13}C NMR spectrum obtained at ambient temperature suggested a fluxional behavior of **8**,¹⁷ which was analyzed by means of variable-temperature ^{13}C NMR spectroscopy

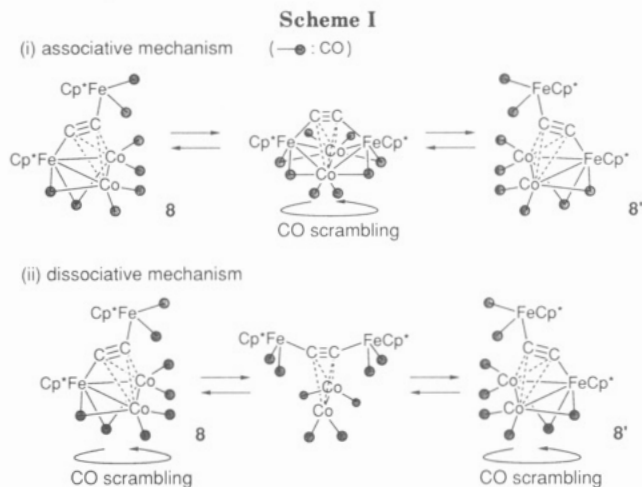


(Figure 3). As a result, as the temperature was brought below -40°C the C_5Me_5 signal broadened, and further cooling below -60°C resulted in the appearance of two sharp C_5Me_5 signals and six singlets. Splitting of the $\text{C}_5(\text{CH}_3)_5$ signal was also observed by ^1H NMR spectroscopy (at 500 MHz) below -60°C . The six ^{13}C NMR signals appearing in the region of δ 150–250 have been assigned as follows. The two intense signals at 215.4 and 250.7 ppm are readily assigned to $\text{Fe}-\text{CO}$ (Fp^*) and $\mu-\text{CO}$, respectively, by comparison with related compounds. The two slightly broad signals are attributed to the carbonyl ligands attached to Co with a quadrupole moment. Then, the remaining two signals at 207.7 and 154.4 ppm have been assigned to C1 and C2 of the quadruply bridging C_2 ligand, respectively. Similar chemical shift values have been reported for the bridging $\mu_3-\eta^1:\eta^2:\eta^2$ -acetylide ligands ($\delta_{\text{C}1}, \delta_{\text{C}2}$): $[\text{Fe}_3(\text{CO})_9(\mu_3-\text{C}_2-\text{Fp})]^-$ (172.9, 132.2),¹⁶ $\text{Fe}_3(\mu_3-\text{C}_2\text{Bu}^t)(\mu-\text{SBU}^t)(\text{CO})_9$ (215.4, 149.49),^{18a} $\text{Fe}_2\text{M}(\mu_3-\text{C}_2\text{R})(\text{CO})_8\text{Cp}$ ($\text{M} = \text{W}, \text{R} = p\text{-Tol}$, 172.9, 112.7; $\text{M} = \text{W}, \text{R} = \text{Me}$, 165.7, 108.3; $\text{M} = \text{Mo}, \text{R} = \text{Me}$, 181.8, 95.9),^{18b} $\text{CpNiFe}_2(\text{CO})_5(\text{L})(\mu_3-\text{C}_2\text{Bu}^t)$ (192.0, 141.0 ($\text{L} = \text{CO}$); 219.4, 136.2 ($\text{L} = \text{PPh}_3$)).^{18c} Thus, a ^{13}C NMR spectrum consistent with the solid-state structure has been obtained at low temperature.

This variable-temperature ^{13}C NMR study has revealed that, at higher temperatures, the two Cp^*Fe parts are observed equivalently and all the CO ligands on both the remote Fe atom and the FeCo_2 cluster core exchange at a rate comparable to the NMR time scale. Attempts to obtain a spectrum at the fast exchange limit were unsuccessful because of thermal decomposition ($>60^\circ\text{C}$). The fluxional behavior of **8** may be explained by a combination of cluster skeletal rearrangement and CO scrambling, and two possible mechanisms, that is, an associative (i) and a dissociative mechanism (ii), are shown in Scheme I. In the associative mechanism (i) the remote Fe atom interacts with FeCo_2 cluster part to form an intermediate with an Fe_2Co_2 butterfly structure. Successive extrusion of the Fp^* group via metal-metal bond scission may regenerate **8**. In this mechanism CO scrambling may take place at the stage of the butterfly intermediate. This associative mechanism

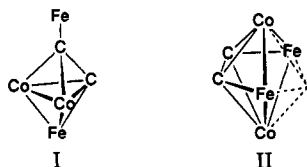
(18) (a) Seyferth, D.; Hoke, J. B.; Rheingold, A. L.; Cowie, M.; Hunter, A. D. *Organometallics* 1988, 7, 2163. (b) Green, M.; Marsden, K.; Salter, I. D.; Stone, F. G. A.; Woodward, P. *J. Chem. Soc., Chem. Commun.* 1983, 446. (c) Sappa, E. *J. Organomet. Chem.* 1987, 323, 83. Although a lot of trinuclear $\mu_3-\eta^1:\eta^2:\eta^2$ -acetylide clusters^{1b} have been structurally characterized and the fluxional behavior of CO and PR_3 ligands has been studied, the ^{13}C NMR data for the acetylide ligands have been reported for only limited examples. See also: (d) Carty, A. *J. Pure Appl. Chem.* 1982, 54, 113. (e) Carty, A. J.; Cherkas, A. A.; Randall, L. H. *Polyhedron* 1988, 7, 1045.

(15) Akita, M.; Moro-oka, Y. Unpublished results.

(16) Jensen, M. P.; Sabat, M.; Shriver, D. F. *J. Cluster Sci.* 1990, 1, 75.

(17) In ref 10 Beck et al. reported that no characterizable ^{13}C NMR spectrum had been obtained for the dirhenium analogue (**9**). Our result suggests that a fluxional mechanism similar to that for **8** may operate for **9**.

may be better described as an interconversion of a closo trigonal-bipyramidal cluster of C_3 symmetry (I) with a nido pentagonal-bipyramidal cluster of C_{2v} symmetry (II), as suggested by one of the reviewers. Both structures have



68 cluster core electrons (I: 52 (the closo trigonal-bipyramidal FeCo_2C_2 cluster) + 16 (the spiked Fp^* group) = 68). On the other hand, in the dissociative mechanism (ii) cleavage of metal-metal bonds proceeds to generate a coordinatively unsaturated intermediate, which is subsequently trapped by either of the two Fp^* groups. If the CO ligands on the FeCo_2 cluster part scramble at a rate much faster than the skeletal rearrangement, all the CO ligands in 8 may be observed equivalently at the fast exchange limit. It is difficult to discriminate between these two mechanisms by NMR experiments alone. However, since the coordinatively unsaturated intermediate could not be trapped by added phosphine, the associative mechanism appears to be preferable.

It should be noted that, in any case, the above mechanisms involve the cluster skeleton rearrangement via a metal-metal bond scission and recombination process in addition to the CO scrambling. While a number of examples of fluxional cluster compounds have been reported so far, in most cases fluxional behavior originates from a fast movement of ligands such as CO on a cluster skeleton. Examples of late-transition-metal cluster compounds which are fluxional by way of a reversible metal-metal bond scission and recombination process are quite rare.¹⁹

Conclusion

Introduction of Fp and Fp^* groups as a substituent (R) of the dicobalt-alkyne adduct $\text{Co}_2(\text{CO})_6(\mu-\eta^2-\eta^2-\text{R}-\text{C}\equiv\text{C}-\text{H})$ does not significantly perturb the electronic structure of the tetrahedral C_2Co_2 core. On the other hand, the reaction of the ethynediyliron complex 7 with $\text{Co}_2(\text{CO})_8$ leads to the formation of the tetranuclear adduct with a quadruply bridging $\mu_4-\text{C}_2$ ligand (8) via an additional interaction between the Fp^* substituent and the Co_2 part. The resulting adduct (8) exhibits fluxional behavior by way of a reversible metal-metal bond scission and recombination process.

Thus, the C_2H and C_2 ligands (C_2 ligands) in 1, 2, and 7 can bind up to four metal centers together through σ and π bonds, and the interaction modes and the fluxional behavior of the C_2 ligands in the formed polymetallic environment provide information on chemical properties of the corresponding surface-bound C_2 species. Such carbon-rich C_2 hydrocarbonyl species may be formed at an early stage of catalytic CO hydrogenation. In contrast to the plentiful chemistry of C_1 species, the chemistry of C_2 species appears to remain much less developed. Further studies of adduct formation of 1, 2, and 7 with mono- and

polymetallic species are now underway.

Experimental Section

General Considerations. All manipulations were carried out under an argon atmosphere by using standard Schlenk-tube techniques.

THF, ether, and hexanes (Na-K/benzophenone) and CH_2Cl_2 (P_2O_5) were treated with appropriate drying agents, distilled, and stored under an argon atmosphere. Deuterated solvents for NMR spectroscopy containing 0.5% TMS as an internal standard were dried over molecular sieves and distilled under reduced pressure. $\text{Fp}-\text{C}\equiv\text{C}-\text{H}$ was prepared by the reaction of $\text{Fp}-\text{I}$ with $\text{H}-\text{C}\equiv\text{C}-\text{MgBr}$.^{2b} $\text{Fp}^*-\text{C}\equiv\text{C}-\text{H}$ and $\text{Fp}^*-\text{C}\equiv\text{C}-\text{Fp}^*$ were prepared according to the methods described in our previous paper.^{2a} $\text{Co}_2(\text{CO})_8$ was purchased from Kanto Chemicals and used as received.

¹H and ¹³C NMR spectra were recorded on JEOL GX-270 and JEOL GX-500 spectrometers (the former spectrometer was used unless otherwise stated: ¹H, 270 MHz; ¹³C, 67.9 MHz). IR and FD-MS spectra were obtained on a Hitachi 260-50 spectrometer and a Hitachi M-80 mass spectrometer, respectively.

Interaction of $\text{Fp}-\text{C}\equiv\text{C}-\text{H}$ (1) with $\text{Co}_2(\text{CO})_8$ (Preparation of 3). To a THF solution (13 mL) of $\text{Co}_2(\text{CO})_8$ (524 mg, 1.53 mmol) was added 1 (309.5 mg, 1.53 mmol) in small portions. Upon addition the reaction mixture turned green with gas evolution. After the mixture was stirred for 1.5 h at room temperature, the volatiles were removed under reduced pressure. The deep green residue was extracted with hexanes, and the extracts were filtered through an alumina pad (2 cm \times 2 cm, activity II-IV; Merck Art. No. 1097), which was successively washed with a minimum amount of CH_2Cl_2 . Concentration of the filtrate followed by crystallization at -20°C gave 3 as deep green crystals (625 mg, 1.28 mmol) in 83% yield. 3: ¹H NMR (CDCl_3 , 27°C) δ 5.01 (s, 5 H, Cp), 6.33 (s, 1 H, C_2H); ¹³C NMR (CDCl_3 , 27°C) δ 87.8 (d, ¹ $J_{\text{CH}} = 180.1$ Hz, Cp), 95.7 (d, ¹ $J_{\text{CH}} = 218.8$ Hz, C2), 102.2 (d, ² $J_{\text{CH}} = 14.7$ Hz, C1), 202.1 (br s, Co-CO), 213.4 (s, Fe-CO); IR (KBr) $\nu(\text{C}\equiv\text{O})$ 2060, 2011, 1986, 1961 cm^{-1} ; FDMS m/z 487 (M^+). Anal. Calcd for $\text{C}_{15}\text{H}_6\text{O}_8\text{FeCo}_2$: C, 37.50; H, 1.04. Found: C, 37.05; H, 1.15.

Interaction of $\text{Fp}^*-\text{C}\equiv\text{C}-\text{H}$ (2) with $\text{Co}_2(\text{CO})_8$ (Preparation of 4). In a manner similar to the reaction of 1, 2 (1.32 g, 3.85 mmol) and $\text{Co}_2(\text{CO})_8$ (1.05 g, 3.85 mmol) were reacted in THF (30 mL) for 1 h at room temperature. The residue was extracted with hexanes, and the extracts were filtered through an alumina pad (2 cm \times 2 cm). Addition of a small amount of ether followed by crystallization at -20°C afforded 4 as dark green crystals (1.51 g, 2.70 mmol) in 70% yield. 4: ¹H NMR (CDCl_3 , 27°C) δ 1.83 (s, 15 H, Cp*), 6.47 (s, 1 H, C_2H); ¹³C NMR (CDCl_3 , 27°C) δ 9.8 (q, ¹ $J_{\text{CH}} = 128.2$ Hz, C_5Me_5), 92.6 (d, ¹ $J_{\text{CH}} = 218.2$ Hz, $\text{C}\equiv\text{C}-\text{H}$), 97.0 (s, C_5Me_5), 109.5 (d, ² $J_{\text{CH}} = 16.8$ Hz, C1), 202.7 (br s, Co-CO), 215.2 (s, Fe-CO); IR (KBr) $\nu(\text{C}\equiv\text{O})$ 2069, 2008, 1994, 1968, 1956 cm^{-1} ; FDMS m/z 558 (M^+). Anal. Calcd for $\text{C}_{20}\text{H}_{16}\text{O}_8\text{FeCo}_2$: C, 43.04; H, 2.89. Found: C, 42.91; H, 2.73.

Interaction of $\text{Fp}^*-\text{C}\equiv\text{C}-\text{Fp}^*$ (7) with $\text{Co}_2(\text{CO})_8$ (Preparation of 8). In a manner similar to the reaction of 1, 7 (417 mg, 0.80 mmol) and $\text{Co}_2(\text{CO})_8$ (275 g, 0.80 mmol) were reacted in THF (15 mL) for 3 h at room temperature. After the completion of the reaction was checked by TLC (alumina), the residue was extracted with ether and the extracts were filtered through an alumina pad (2 cm \times 2 cm), which was washed with a minimum amount of CH_2Cl_2 . Concentration of the filtrate followed by crystallization at -20°C afforded 8 as dark green microcrystals (440 mg, 0.59 mmol) in 73% yield. 8: ¹H NMR (CDCl_3 , 27°C) δ 1.75 (s, Cp*); ¹H NMR (CD_2Cl_2 , -80°C , at 500 MHz) δ 1.67, 1.75 (s \times 2, 2 Cp*); ¹³C NMR (CDCl_3 , 27°C) δ 9.4 (C_5Me_5), 96.8 (s, C_5Me_5); ¹³C NMR (CD_2Cl_2 , -80°C) δ 9.6, 9.8 (C_5Me_5), 96.7, 98.0 (C_5Me_5), 154.4 (C2), 203.4 (Co-CO), 207.7 (C1), 213.4 (Co-CO), 215.4 (Fe-CO), 250.7 (μ -CO); IR (KBr) $\nu(\text{C}\equiv\text{O})$ 1990, 1961, 1952, 1813 cm^{-1} ; FDMS m/z 748 (M^+). Anal. Calcd for $\text{C}_{30}\text{H}_{30}\text{O}_8\text{Fe}_2\text{Co}_2$: C, 48.16; H, 4.04. Found: C, 47.58; H, 4.09.

Single-Crystal X-ray Diffraction Study. Suitable crystals of 3 and 8 were obtained by recrystallization from an ether-hexane mixed solvent system and mounted on glass fibers. Diffraction measurements were made on a Rigaku AFC-5 automated four-circle diffractometer by using graphite-monochromated $\text{Mo K}\alpha$ radiation ($\lambda = 0.71058 \text{ \AA}$). Unit cells were determined and refined

(19) Transition-metal clusters containing a group 11 metal component(s) frequently exhibit fluxional behavior via an M-M bond scission and recombination: (a) Salter, I. D. *Adv. Dynamic Stereochem.* 1989, 2, 57. (b) Salter, I. D. *Adv. Organomet. Chem.* 1990, 29, 249. However, examples of other group metal clusters are still quite rare. (c) Farrugia, L. J. *Adv. Organomet. Chem.* 1990, 31, 301. (d) Houser, E. J.; Amarakkera, J.; Rauchfuss, T. B.; Wilson, S. R. *J. Am. Chem. Soc.* 1991, 113, 7440. (e) References cited in ref 19b.

by a least-squares method using 25 independent reflections with $20^\circ < 2\theta < 25^\circ$ (3) and $12^\circ < 2\theta < 20^\circ$ (8). Data were collected with the ω - 2θ scan technique. If $\sigma(F)/F$ was more than 0.1, a scan was repeated up to three times and the results were added to the first scan. Three standard reflections were monitored at every 100 measurements. All data processing was performed on a FACOM A-70 computer by using the R-CRYSTAN structure solving program system obtained from Rigaku Corp., Tokyo, Japan. Neutral scattering factors were obtained from the standard sources.²⁰ In the reduction of data, Lorentz and polarization corrections were made and no absorption correction was made. Full-matrix least-squares refinement minimized the function $[\sum w(|F_o| - |F_c|)^2 / \sum w|F_o|^2]^{1/2}$, where $w = 1/[\sum (F_o)^2 + (pF_c)^2]$, the parameter p being automatically optimized.

3 and 8 crystallized in a triclinic and monoclinic system, respectively. The positions of the metal atoms were located by direct methods (SAPI 85). Subsequent difference Fourier maps revealed the positions of all the non-hydrogen atoms. For 3 all the non-hydrogen atoms were refined anisotropically, and the positions

of the hydrogen atoms were confirmed by using isotropic thermal parameters with $B(H) = B(C)$. For 8 the non-hydrogen atoms other than the Cp* groups were refined anisotropically and the carbon atoms of the Cp* groups were refined isotropically, because enough data could not be obtained owing to the small size of the crystal.

Acknowledgment. We are grateful to Prof. D. F. Shriver for sending us a reprint of ref 16. This research was financially supported by a Grant-in-Aid from the Ministry of Education, Science, and Technology of the Japanese Government.

Registry No. 1, 33029-77-5; 2, 125453-83-0; 3, 140362-50-1; 4, 140362-51-2; 7, 134153-80-3; 8, 140362-52-3; Co₂(CO)₈, 10210-68-1; Fe, 7439-89-6; CO, 7440-48-4.

Supplementary Material Available: Tables of anisotropic thermal parameters and bond lengths and angles for 3 and 8 (13 pages). Ordering information is given on any current masthead page.

OM910711T

(20) *International Tables for X-ray Crystallography*; Kynoch Press: Birmingham, U.K., 1975; Vol. 4.

Sterically Crowded Aryloxy Compounds of Aluminum: Reduction of Coordinated Benzophenone

Michael B. Power, John R. Nash, Matthew D. Healy, and Andrew R. Barron*

Department of Chemistry, Harvard University, Cambridge, Massachusetts 02138

Received December 19, 1991

The interaction of AlEt(BHT)₂ with benzophenone, O=CPh₂, in pentane or benzene yields as the sole product Al(BHT)₂(OCHPh₂)(O=CPh₂) (1). In diethyl ether, however, the Lewis acid-base complex AlEt(BHT)₂(O=CPh₂) (2) is isolated. Thermolysis of 2 yields Al(BHT)₂(OCHPh₂) (3), which reacts rapidly with Et₂O, THF, or O=CPh₂ to give the acid-base complexes Al(BHT)₂(OCHPh₂)(L) (L = Et₂O (4), THF (5), O=CPh₂ (1)). Interaction of AlEt₂(BHT)(OEt₂) with 1 equiv of benzophenone in diethyl ether produces the isolable complex AlEt₂(BHT)(O=CPh₂) (6). Solid-phase thermolysis of 6 yields the monomer AlEt(BHT)(OCHPh₂) (7), which dimerizes upon dissolution in organic solvents to give [AlEt(BHT)(μ-OCHPh₂)]₂ (8). In the presence of excess benzophenone in benzene solution, AlEt₂(BHT)(OEt₂) gives AlEt(BHT)(OCHPh₂)(O=CPh₂) (9), which rearranges when heated in hexane to the bridged dimer (BHT)(Et)Al(μ-OCHPh₂)₂Al(OCHPh₂)(Et) (10). Thermolysis of 7 in the presence of excess benzophenone results in the reduction of a second ketone to give Al(BHT)(OCHPh₂)₂(O=CPh₂) (11). Unlike the benzophenone derivatives, the reaction of acetophenone with AlEt(BHT)₂ and AlEt₂(BHT)(OEt₂) does not result in ketone reduction but rather in the formation of the thermally stable Lewis acid-base adducts AlEt(BHT)₂[O=C(Me)Ph] (12) and AlEt₂(BHT)[O=C(Me)Ph] (13), respectively. The solvent-dependent formation of the benzophenone adducts 2 and 6 has been related to the solution equilibria and the relative metal-ligand bond dissociation energies (the BDE's) of the methyl compounds AlMe(BHT)₂L (L = Et₂O, THF, py, O=CPh₂, O₂N-C₆H₄-*p*-Me) and 1 which have been obtained from variable-temperature ¹H NMR data. The kinetics of the conversion of 2 to 1 and 9 to 11 have been investigated and the ΔH[‡] and ΔS[‡] values determined. Interaction of 2,6-diphenylphenol (DPP-H) with AlR₃ in a 1:1 molar ratio allows for the isolation of the dimeric compounds [R₂Al(μ-DPP)]₂ (R = Me (14), Et (15)). The reaction of 15 with O=CPh₂ results after hydrolysis in the formation of approximately 1 equiv of HOCHPh₂ per aluminum; however, no intermediate could be isolated.

Introduction

Organoaluminum compounds undergo a wide range of reactions with organic carbonyls.¹ Much of their reactivity, including the undesirable presence of multiple reaction pathways, is dependent on the dimeric nature of many organoaluminum compounds. In order for future development of new organoaluminum compounds with a broad synthetic utility to be possible, a detailed knowledge

of their mechanisms and the factors controlling product distribution is required. Toward this end, recent work in our laboratory has explored the reactivity of organic carbonyls with monomeric aluminum complexes derived from the sterically hindered phenol 2,6-di-*tert*-butyl-4-methylphenol (BHT-H, from the trivial name butylated hydroxytoluene).²⁻⁷

* To whom correspondence should be addressed.

(1) Zietz, J. R.; Robinson, G. C.; Lindsay, K. L. In *Comprehensive Organometallic Chemistry*; Wilkinson, G., Stone, F. G. A., Abel, E. W., Eds.; Pergamon Press: Oxford, England, 1983; Vol. 6, Chapter 46.